nature medicine

Regulation of angiogenesis by tissue factor cytoplasmic domain signaling

Mattias Belting[1,7], Michael I Dorrell[2,7], Staffan Sandgren[3], Edith Aguilar[2], Jasimuddin Ahamed[1], Andrea Dorfleutner[1,6], Peter Carmeliet[4], Barbara M Mueller[5], Martin Friedlander[2] & Wolfram Ruf[1]

Hemostasis initiates angiogenesis-dependent wound healing, and thrombosis is frequently associated with advanced cancer. Although activation of coagulation generates potent regulators of angiogenesis, little is known about how this pathway supports angiogenesis *in vivo*. Here we show that the tissue factor (TF)-VIIa protease complex, independent of triggering coagulation, can promote tumor and developmental angiogenesis through protease-activated receptor-2 (PAR-2) signaling. In this context, the TF cytoplasmic domain negatively regulates PAR-2 signaling. Mice from which the TF cytoplasmic domain has been deleted (TFΔCT mice) show enhanced PAR-2-dependent angiogenesis, in synergy with platelet-derived growth factor BB (PDGF-BB). Ocular tissue from diabetic patients shows PAR-2 colocalization with phosphorylated TF specifically on neovasculature, suggesting that phosphorylation of the TF cytoplasmic domain releases its negative regulatory control of PAR-2 signaling in angiogenesis. Targeting the TF-VIIa signaling pathway may thus enhance the efficacy of angiostatic treatments for cancer and neovascular eye diseases.

Angiogenesis, the formation of new vessels from pre-existing vasculature, has a crucial role during normal development, tissue regeneration in wound healing and postischemic tissue repair. Neovascularization during tumor expansion and in ischemic retinopathies is an example of angiogenesis-driven disease progression[1,2]. An increased understanding of the basic mechanisms that regulate physiological and pathological angiogenesis will aid the development of efficient pro- and antiangiogenic therapies[3,4]. TF initiates the coagulation protease cascade that generates proteolytic fragments with potent regulatory effects on angiogenesis[5]. TF acts as an extracellular coreceptor that activates and presents coagulation proteases for signaling through G-protein-coupled PARs[6]. The PARs are activated through a unique mechanism that involves extracellular proteolysis of the receptor[7,8]. The TF-VIIa complex, as well as Xa, activate PAR-2 *in vitro*. Xa can also cleave PAR-1, the first identified thrombin receptor. Xa signals most efficiently in the ternary TF-VIIa-Xa complex[9,10].

In vitro data suggest that TF acts as a coreceptor in PAR signaling, but the role of the TF cytoplasmic domain in PAR signaling *in vivo* remains poorly defined. TF expressed by tumor cells contributes to tumor progression. Upregulation of vascular endothelial cell growth factor (VEGF) by the TF cytoplasmic domain has been suggested[11], although not widely confirmed[12], to contribute to pathological angiogenesis. In addition, TF localizes to the endothelium in malignant breast cancer[13], and direct inhibitors of TF suppress tumor growth and angiogenesis[14]. PAR-1 and PAR-2 have also been implicated in angiogenesis[15,16], but *in vivo* data linking angiogenesis to PAR activation by TF-initiated coagulation remain sparse[17].

RESULTS

Deletion of TF cytoplasmic domain enhances angiogenesis

To evaluate the role of the TF cytoplasmic domain in tumor angiogenesis, we studied the growth of syngeneic tumors in TFΔCT mice, in comparison to their wild-type littermates (**Fig. 1a**). Tumor expansion and final tumor weight were approximately twofold higher in TFΔCT than in wild-type mice. Tumors from wild-type and TFΔCT mice had similar end-stage vessel densities (**Fig. 1a**), consistent with the notion that tumor expansion followed increased blood supply[4] and that the tumor cells established similar neovasculatures in these mice. However, these data did not exclude the possibility that TF expressed by host stromal cells might contribute to accelerated angiogenesis in TFΔCT mice. To directly analyze the regulatory role of the TF cytoplasmic domain in vascular cells under defined conditions, we used the aortic ring assay, which was carried out in the presence of autologous mouse serum to stimulate angiogenesis[18]. Microvessel sprouting from TFΔCT mouse aortas was twofold higher relative to wild-type aortas (**Fig. 1b,c**). Aortic sprout cells were primarily endothelial, as shown by positive staining for CD31 and negative staining for smooth

[1]Department of Immunology and [2]Department of Cell Biology, The Scripps Research Institute, 10550 North Torrey Pines Road, La Jolla, California 92037, USA. [3]Biomedical Centre, C-13, Lund University, SE-221 84 Lund, Sweden. [4]Flanders Interuniversity Institute for Biotechnology, University of Leuven, Leuven, Belgium, B-3000. [5]Division of Cancer Biology, La Jolla Institute for Molecular Medicine, 4570 Executive Drive, San Diego, California 92121, USA. [6]Present address: The Mary Babb Randolph Cancer Center and the Department of Microbiology and Immunology, West Virginia University, Morgantown, West Virginia 26506, USA. [7]These authors contributed equally to this work. Correspondence should be addressed to W.R. (ruf@scripps.edu) or M.F. (friedlan@scripps.edu).

Published online 18 April 2004; doi:10.1038/nm1037

muscle cell actin (SMA; **Fig. 1b**). We observed similar TF expression levels in sprouting TFΔCT and wild-type aortas (**Fig. 1d**), indicating that loss of the TF cytoplasmic tail, rather than deregulated TF expression, caused accelerated endothelial cell sprouting in TFΔCT mice.

Because TF cytoplasmic domain signaling has been implicated in regulating VEGF expression by tumor cells[11], we tested whether wild-type aortas show reduced sprouting because of a relative deficiency in VEGF. Supplementing serum with VEGF did not abolish the difference in sprouting from TFΔCT compared with wild-type aortas (**Fig. 2a**). Aortas stimulated with VEGF in the absence of serum showed very limited sprouting, however, indicating that serum was required for accelerated angiogenesis from TFΔCT aortas (**Fig. 2a**). Sprouting from wild-type aortas in the presence of TFΔCT mouse serum (serum swap) was not enhanced, indicating that TF expressed by TFΔCT vascular cells, rather than a serum factor or increased levels of circulating TF, confers the proangiogenic phenotype (**Fig. 2a**).

TF-VIIa signaling accelerates angiogenesis in TFΔCT aortas

The serum dependence of the TFΔCT sprouting phenotype suggested that genetic ablation of the TF cytoplasmic tail may unmask coagulation factor-dependent proangiogenic activity. We therefore studied the inhibitory effects of blocking coagulation proteases in the aortic ring sprouting model (**Fig. 2b**). Inhibition of thrombin by hirudin, as well as inactivation of Xa by nematode anticoagulant peptide-5 (NAP-5), had no effect on sprouting, thereby excluding contribution from proteases downstream in the coagulation cascade. Active site–inhibited VIIa (VIIai), a high-affinity competitive antagonist that blocks TF-VIIa complex formation, as well as NAP-c2, which inhibits TF-VIIa by forming a trapped TF-VIIa-Xa complex, reversed the TFΔCT sprouting phenotype but did not influence sprouting from wild-type aortas. The combination of NAP-c2 and NAP-5 had an effect similar to that of NAP-5 alone, excluding the possibility that Xa, which can signal in the NAP-c2-trapped TF-VIIa-Xa complex[10], unexpectedly suppressed the TFΔCT phenotype. These results suggest that the TF cytoplasmic domain negatively regulates TF-VIIa protease signaling.

To directly analyze the role of VIIa in angiogenesis, we replaced serum with VIIa in the aortic ring model. VIIa inefficiently induced sprouting from both wild-type and TFΔCT aortas (**Fig. 2c**). Because endothelial cell sprouting is typically dependent on growth factor signaling, we further characterized sprouting from TFΔCT aortas in the presence of the defined proangiogenic growth factors VEGF, PDGF-AA, PDGF-BB and basic fibroblast growth factor (FGF). None of these factors promoted substantial sprouting, which is consistent with previous data[18], and the proangiogenic phenotype of TFΔCT was not apparent in the presence of any of the growth factors alone. However, combining VIIa with PDGF-BB selectively recapitulated the proangiogenic phenotype of TFΔCT observed under serum conditions (**Fig. 2c**). There was no evidence for an additive effect of PDGF-BB and VIIa on sprouting from wild-type aortas, as described for fibroblast migration[19]. PDGF-AA is a selective agonist for PDGF receptor-α but cannot activate PDGF receptor-β. Because VIIa enhanced angiogenesis in the presence of PDGF-BB, but not PDGF-AA, TF-VIIa signaling seems to synergize with PDGF receptor-β signaling when negative regulatory control by the TF cytoplasmic domain is lost.

TF-VIIa signaling cross-talk with PAR-2 regulates angiogenesis

Because PAR-2 is the primary target for TF-VIIa signaling, we hypothesized that TF-VIIa-dependent PAR-2 activation synergizes with PDGF-BB to accelerate angiogenesis in TFΔCT mice. We used a genetic approach to test our hypothesis. Aortic ring sprouting in TFΔCT mice that are also deficient in PAR-2 reverted to wild-type levels (**Fig. 2d,e**), indicating that loss of the TF cytoplasmic domain leads to PAR-2-dependent accelerated angiogenesis. No alterations in angiogenesis were evident upon deletion of PAR2 alone, suggesting that the TF cytoplasmic tail is highly efficient in suppressing the proangiogenic effects of PAR-2. This was also supported by the finding that TF-directed inhibitors (VIIai and NAP-c2) did not reduce sprouting from wild-type aortas (**Fig. 2b**).

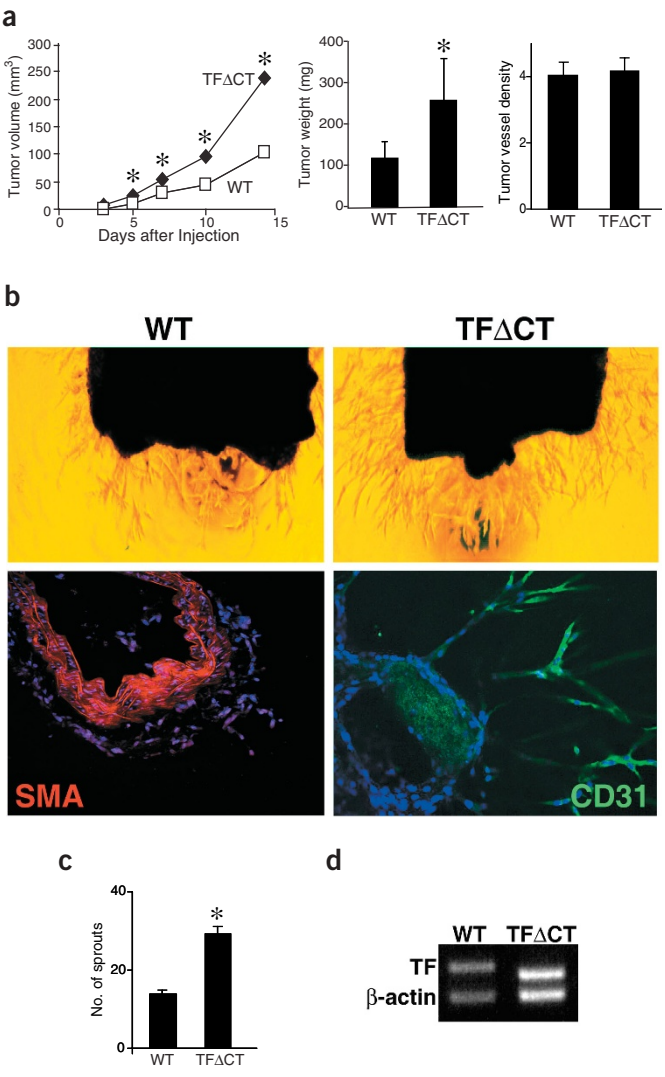

Figure 1 Enhanced tumor growth and angiogenesis in TFΔCT mice. (**a**) Syngeneic T241 fibrosarcoma tumor volumes (left) and final weights (middle) on day 14 in wild-type (WT) and TFΔCT mice ($n = 5$; *, $P < 0.05$ by t test). Enhanced tumor expansion was confirmed with the Lewis lung carcinoma tumor model (data not shown). Right, vessel density of T241 tumors based on CD31 staining. (**b**) *Ex vivo* angiogenesis. Top, representative light microscopy of day 3 wild-type and TFΔCT aortic pieces embedded in Matrigel (original magnification, ×20). Bottom, confocal fluorescence microscopy after staining of wild-type aortic pieces as indicated. Location of cells was visualized by nuclear (TOPRO; blue) staining. Original magnification, ×10. (**c**) Quantitation of sprouting from wild-type and TFΔCT aortas on day 3. Data represent mean ± s.e.m.; $n = 74$; *, $P < 0.05$ by t test. (**d**) Semiquantitative PCR for TF and β-actin on day 4 in wild-type and TFΔCT aortas.

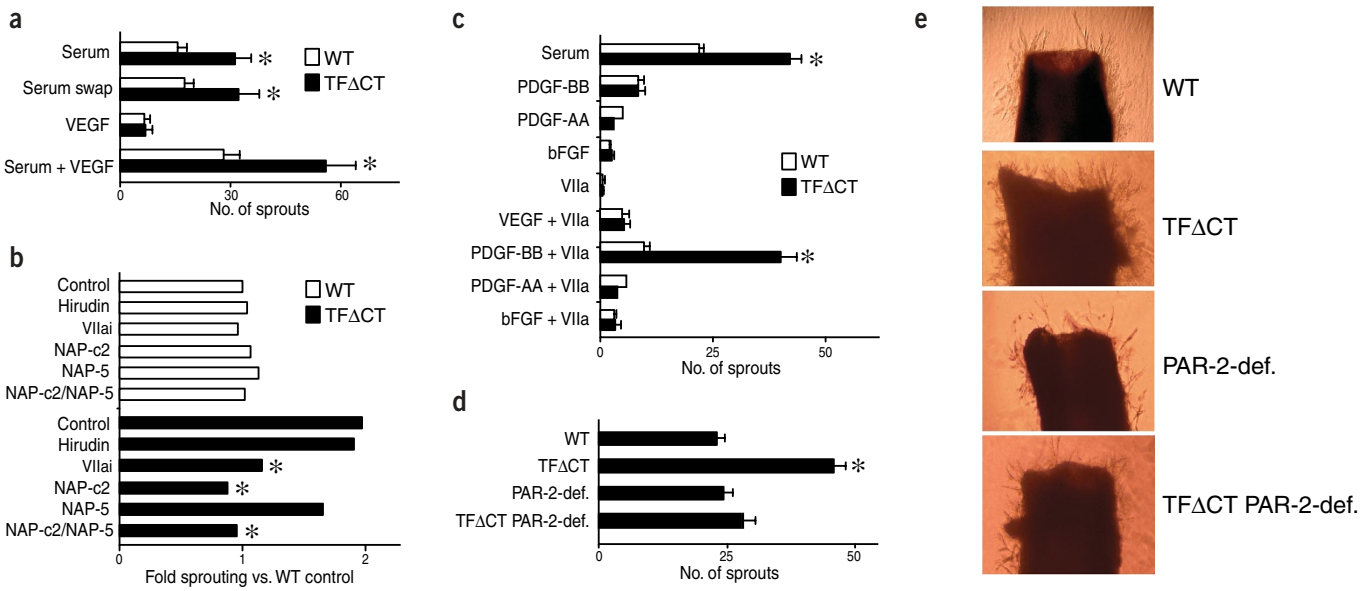

Figure 2 Synergy of TF-VIIa complex and PDGF-BB in angiogenesis. (**a**) Wild-type (WT) and TFΔCT aortic sprouting on day 3 under the indicated conditions. Data represent mean ± s.e.m.; $n = 10–15$; *, $P < 0.05$ by t test. (**b**) Wild-type and TFΔCT aortas were incubated in serum with additional protease inhibitors as indicated for 3 d. *, $P < 0.05$ by t test compared with TFΔCT control. (**c**) Sprouting on day 4 from wild-type and TFΔCT aortas in endothelial cell growth medium supplemented as indicated. Data represent mean ± s.e.m.; $n = 5–19$; *, $P < 0.05$ by t test compared with wild type. (**d**) Enhanced sprouting from TFΔCT aortas requires PAR-2 expression. Wild-type, TFΔCT, PAR-2-deficient and TFΔCT PAR-2-deficient aortic sprouting was measured on day 4. Data represent mean ± s.e.m.; $n = 21–37$; *, $P < 0.05$ by t test compared with wild type. (**e**) Representative aortic pieces from mice of indicated genotypes (original magnification, ×20).

To exclude the possibility that the phenotype of TFΔCT mice is unrelated to TF cytoplasmic domain signaling, we expressed full-length human TF(1–263) or, as a control, cytoplasmic domain–deleted human TF(1–243) by adenoviral transduction in wild-type or TFΔCT aortas. Coexpression of green fluorescent protein (GFP) and staining with human TF-specific antibodies showed that the migration of endothelial sprout cells into the surrounding Matrigel was suppressed by human TF(1–263), but not human TF(1–243) (**Fig. 3a**).

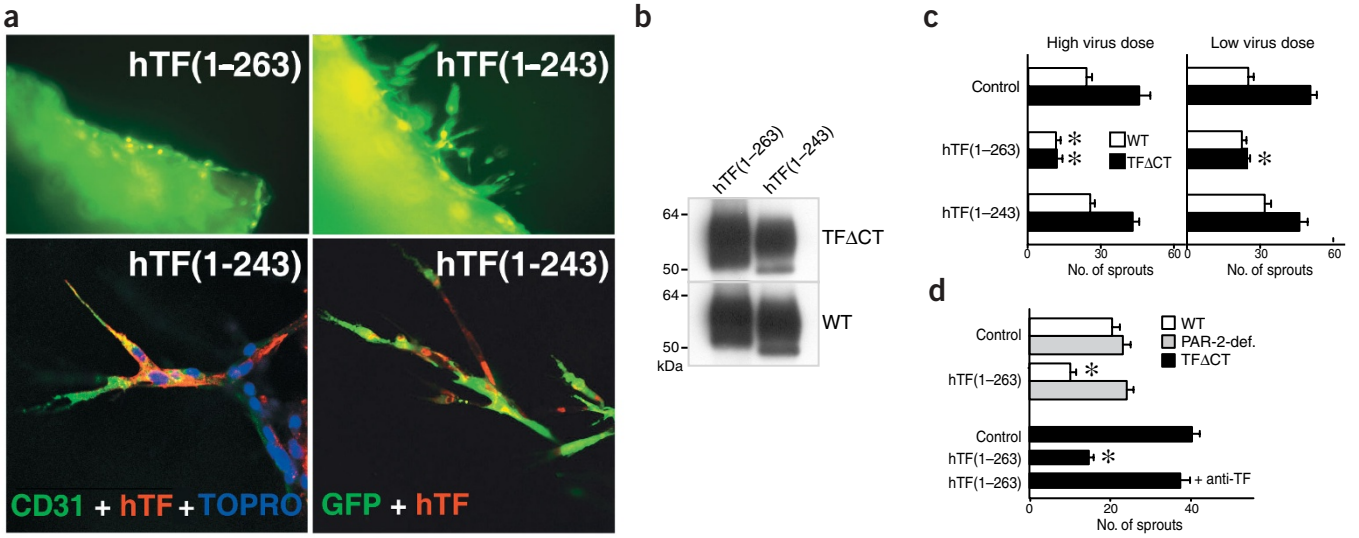

Figure 3 TF cytoplasmic domain suppresses PAR-2-dependent angiogenesis. (**a**) Top, fluorescence microscopy of day 3 TFΔCT aortic pieces cotransduced with GFP and human TF(1–263) or human TF(1–243) at a high viral dose (magnification, ×20). Bottom, confocal fluorescence microscopy of TFΔCT aortic sprouts transduced with human TF(1–243) (left) or human TF(1–243) and GFP (right) and stained as indicated. Nuclei in left panel were visualized by TOPRO staining (magnification, ×10). (**b**) Human TF was immunoprecipitated from detergent extracts of wild-type (WT) or TFΔCT aortic pieces transduced with high viral dose for 4 d, and detected by western blotting with polyclonal antibody to TF. (**c**) Sprouting from wild-type and TFΔCT aortas transduced with human TF(1–263) or human TF(1–243) at a high or low viral dose. Data represent mean ± s.e.m.; $n > 13$; *, $P < 0.05$ by t test compared with control. (**d**) Suppression of sprouting by human TF(1–263) requires PAR-2 expression and TF extracellular activity. Wild-type, TFΔCT and PAR-2-deficient aortas were transduced with high-dose human TF(1–263), then incubated in serum with (+ anti-TF) or without antibodies to the human TF extracellular domain. Number of sprouts was determined on day 4. Data represent mean ± s.e.m.; $n > 17$; *, $P < 0.05$ by t test compared with control.

Colocalization of human TF with CD31 provided evidence for adenoviral transduction of endothelial cells. Western blot analysis of human TF in extracts from aortic ring assays confirmed equal expression levels of both forms of TF (**Fig. 3b**). At a higher dose of virus, human TF(1–263) suppressed sprouting from both wild-type and TFΔCT aortas, whereas TFΔCT sprouting was selectively reversed to wild-type levels by a lower viral dose (**Fig. 3c**). In all cases, truncated human TF(1–243) had no effect, showing that suppression is dependent on the TF cytoplasmic tail (**Fig. 3c**). These data support the concept that, when introduced at the appropriate level, the TF cytoplasmic domain can restore negative regulatory control of PAR-2 signaling in angiogenesis.

To gain further insight into the mechanism by which the TF cytoplasmic domain suppresses PAR-2 signaling in angiogenesis, we tested whether the reversal of the proangiogenic phenotype of TFΔCT aortas requires signaling and extracellular protease assembly with the introduced human TF. Blockade of the extracellular domain of TF(1–263) with human TF-specific monoclonal antibodies prevented the reversal of the enhanced sprouting phenotype of TFΔCT mice (**Fig. 3d**). The involvement of PAR-2 was addressed based on the finding that expression of high levels of human TF(1–263) suppressed sprouting from wild-type aortas. An equivalent virus dose did not reduce sprouting from PAR-2-deficient aortas, indicating that the suppressive function of the TF cytoplasmic domain requires PAR-2 expression (**Fig. 3d**). Collectively, these data show that negative regulatory control of angiogenesis by the TF cytoplasmic domain occurs specifically in the context of PAR-2 signaling.

The TF cytoplasmic domain regulates physiological angiogenesis

To further address the role of the TF cytoplasmic domain *in vivo*, we characterized physiological angiogenesis in the neonatal retina, which develops a vascular network emanating from the optic disc in a stereotypical manner[20]. In neonatal mice, the diameter of the superficial vascular plexus of TFΔCT mice was twice that of wild-type mice, indicating that the TF cytoplasmic tail negatively regulates *in vivo* angiogenesis during postnatal development (**Fig. 4a**). The extent of vascularization in newborn TFΔCT retinas was comparable to that of 2-d-old (P2) wild-type retinas (**Fig. 4b**). Consistent with the data from the aortic ring assay, retinas from neonatal PAR-2-deficient and TFΔCT PAR-2-deficient mice showed age-appropriate vascularization (**Fig. 4a**). The evaluation of at least ten retinas, derived from at least three different pregnancies for each genotype, confirmed the consistency of the observed phenotype of TFΔCT mice and the consistency of its reversal by concomitant deletion of PAR-2 (**Fig. 4c**).

Vascular cell–specific localization of TF in TFΔCT retinas was difficult to evaluate because of the prominent expression of TF by astrocytes, an established TF-expressing cell type in the CNS[21], as well as potential TF expression by the underlying nerve fibers. Glial fibrillary acidic protein (GFAP) staining of astrocytes revealed that astrocytes extended to the periphery of retinas from both wild-type and TFΔCT newborn mice, with no apparent difference in staining patterns (**Fig. 5a**). This result argues that vascular development did not indirectly follow accelerated developmental astrocyte migration in TFΔCT retinas. Vascular apoptosis is infrequently observed in wild-type mice at this stage of development[22], and protection from apoptosis is therefore an unlikely cause for accelerated angiogenesis in TFΔCT mice. Enhanced vascular development may result from increased cell proliferation, but proliferating vascular cells as assessed by Ki-67 staining are present in comparable numbers in both newborn TFΔCT and P2 wild-type retinas (**Fig. 5b,c**). While the degree of peripheral vascular extension was comparable between P0 TFΔCT and P2 wild-type retinas, the degree of arborization was more pronounced in P2 wild-type vascular plexus (**Fig. 4a,b**). This may reflect enhanced TFΔCT endothelial cell migration, consistent with the scaffolding function of PAR-2 that localizes the MAP kinase pathway at the leading edge of migrating cells[23]. TF is expressed in angiogenic endothelial cells associated with malignant breast tumors[13], and *in vitro* studies have shown direct effects of PDGF-BB on primary endothelial cell migration and cord or tube formation through activation of PDGF receptor-β, which is detectable on capillary endothelial cells *in vivo*[24,25].

PDGF-BB signaling is also crucial to the recruitment and expansion of the mural cell and pericyte populations that stabilize and regulate remodeling of the vascular architecture[26–29]. Complete deletion of the gene encoding TF causes defective vascular remodeling of the embryo-

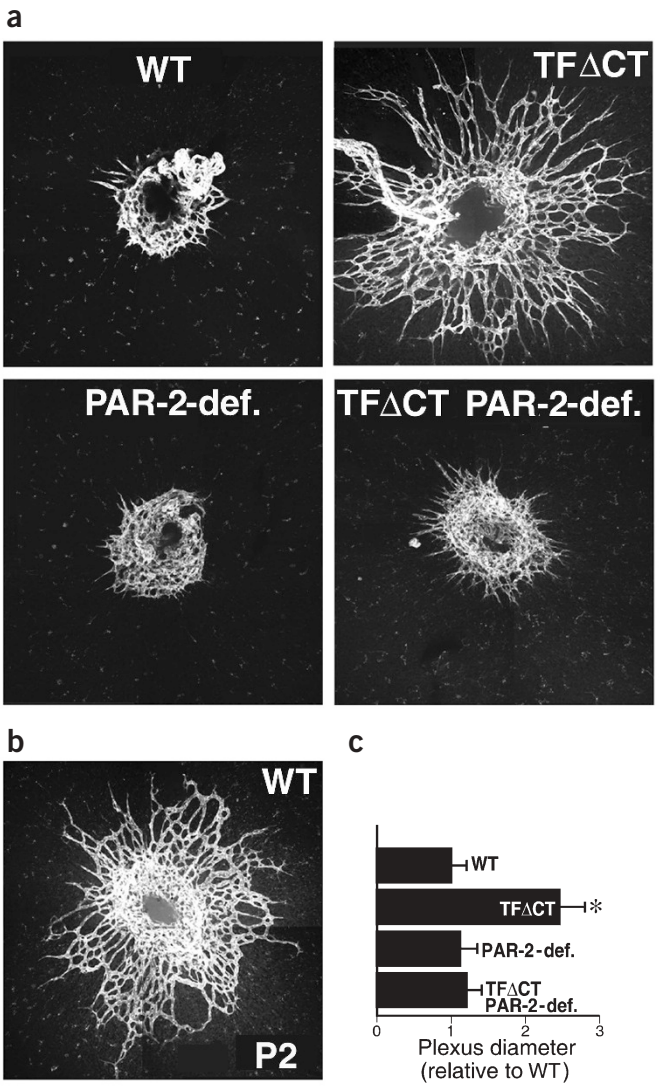

Figure 4 Accelerated developmental angiogenesis in TFΔCT mice. (**a**,**b**) Representative retinas from P0 wild-type (WT), TFΔCT, PAR-2-deficient and TFΔCT PAR-2-deficient mice (**a**). A P2 wild-type retina is shown for comparison (**b**). Vascular plexus were stained with fluorescense-conjugated isolectin *Griffonia simplicifolia*. Images were generated as montages of four individual images taken at ×20 magnification. (**c**) Quantitation of average vascular plexus diameter of P0 retinas from the indicated genotypes. Error bars indicate s.e.m. *, $P < 0.01$ by *t* test, compared with wild type.

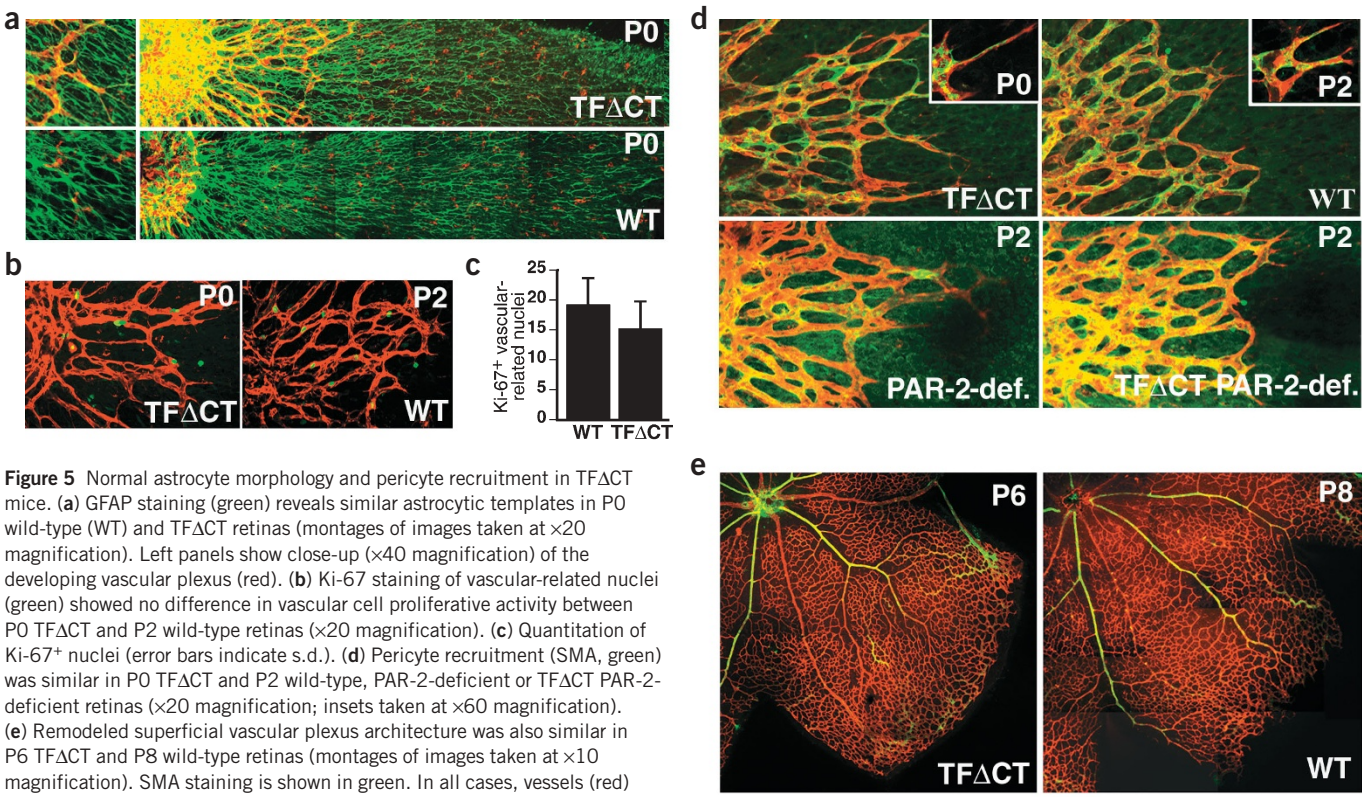

Figure 5 Normal astrocyte morphology and pericyte recruitment in TFΔCT mice. (**a**) GFAP staining (green) reveals similar astrocytic templates in P0 wild-type (WT) and TFΔCT retinas (montages of images taken at ×20 magnification). Left panels show close-up (×40 magnification) of the developing vascular plexus (red). (**b**) Ki-67 staining of vascular-related nuclei (green) showed no difference in vascular cell proliferative activity between P0 TFΔCT and P2 wild-type retinas (×20 magnification). (**c**) Quantitation of Ki-67$^+$ nuclei (error bars indicate s.d.). (**d**) Pericyte recruitment (SMA, green) was similar in P0 TFΔCT and P2 wild-type, PAR-2-deficient or TFΔCT PAR-2-deficient retinas (×20 magnification; insets taken at ×60 magnification). (**e**) Remodeled superficial vascular plexus architecture was also similar in P6 TFΔCT and P8 wild-type retinas (montages of images taken at ×10 magnification). SMA staining is shown in green. In all cases, vessels (red) were visualized by staining with isolectin *Griffonia simplicifolia*.

nic vascular plexus in the yolk sac, with associated reduction in pericyte recruitment[30]. The close association between endothelial and mural cells during angiogenic sprouting makes it challenging to distinguish between autocrine effects of PDGF-BB on endothelial cells and secondary, paracrine effects on recruited mural cells[28,29]. Using SMA staining as a pericyte-specific marker, we observed a similar staining pattern in the retinal vasculature of newborn TFΔCT and P2 wild-type mice (**Fig. 5d**). Pericyte staining in each case extended to the tips of the sprouts (**Fig. 5d**). The vascular plexus of P2 PAR-2-deficient or TFΔCT PAR-2-deficient mice were indistinguishable from those of P2 wild-type mice. These data show that pericyte recruitment is normal in PAR-2-deficient mice, and exclude the possibility that developmental vascular abnormalities of PAR-2 deficiency appear after day P0. Pericytes have important roles in remodeling the developing retinal vascular plexus. The equivalently expanded superficial vascular plexus of P6 TFΔCT and P8 wild-type retinas also showed comparable capillary network density, distribution of arteries and veins, and pattern of SMA staining (**Fig. 5e**). These similarities at later stages of retinal vascularization argue against altered pericyte function. Accelerated vascular development in TFΔCT retinas persisted at least until day P6, when premature endothelial cell sprouting into the deeper layers of the retina was observed. Collectively, these data are consistent with a phenotype of accelerated endothelial cell migration in the development of the superficial vascular plexus in TFΔCT mice, rather than abnormal pericyte recruitment.

TF phosphorylation in neovascular eye disease

A role for TF in pathological angiogenesis is suggested by the association of TF with the endothelium in malignant breast cancer[13]. The TF cytoplasmic domain is typically unphosphorylated in endothelial cells[31]. We hypothesized that phosphorylation may release the negative regulatory effects of the TF cytoplasmic domain and thus promote pathological angiogenesis. To determine whether TF phosphorylation occurs in pathological angiogenesis, we analyzed specimens of neovascularized iris that were removed from diabetic patients. Indeed, staining with an antibody[31] that specifically recognizes TF phosphorylated at Ser258 identified TF cytoplasmic domain phosphorylation only at sites of neovascularization in specimens from six different patients (**Fig. 6a–c**). TF phosphorylation in these pathological vessels colocalized with PAR-2 expression (**Fig. 6a**), supporting a role for deregulated PAR-2 signaling during pathological neovascularization. Notably, phosphorylated TF and PAR-2 staining were not observed in control iris samples from a glaucoma patient with no history of diabetes or pathological neovascularization (**Fig. 6d**). TF phosphorylation and PAR-2 upregulation were also observed specifically in neovessels in a retina obtained from a patient with diabetic retinopathy. Staining with an antibody to the TF extracellular domain revealed widespread expression of TF in glial and neuronal cell types, mature vessels and at sites of neovascularization (**Fig. 6e**), although TF phosphorylation was observed only in dilated pathological vessels (**Fig. 6e**). Staining of phosphorylated TF in pathological vessels was completely eliminated by competition with the antigenic peptide (**Fig. 6a,f**). Nonspecific punctate staining that was incompletely competed by the immunogen was sometimes observed in the inner and outer limiting membranes, regions noted for nonspecific staining by different antibodies in retina specimens. TF phosphorylation was never observed on normal, mature retinal vessels, supporting a specific role for TF phosphorylation during pathological neovascularization. In serial sections, pronounced PAR-2 expression was observed specifically in the same vessels in which TF phosphorylation was observed (**Fig. 6f**). To confirm that TF phosphorylation was specific to neovessels, we stained diabetic retinas for $\alpha_v\beta_3$-integrin, a known

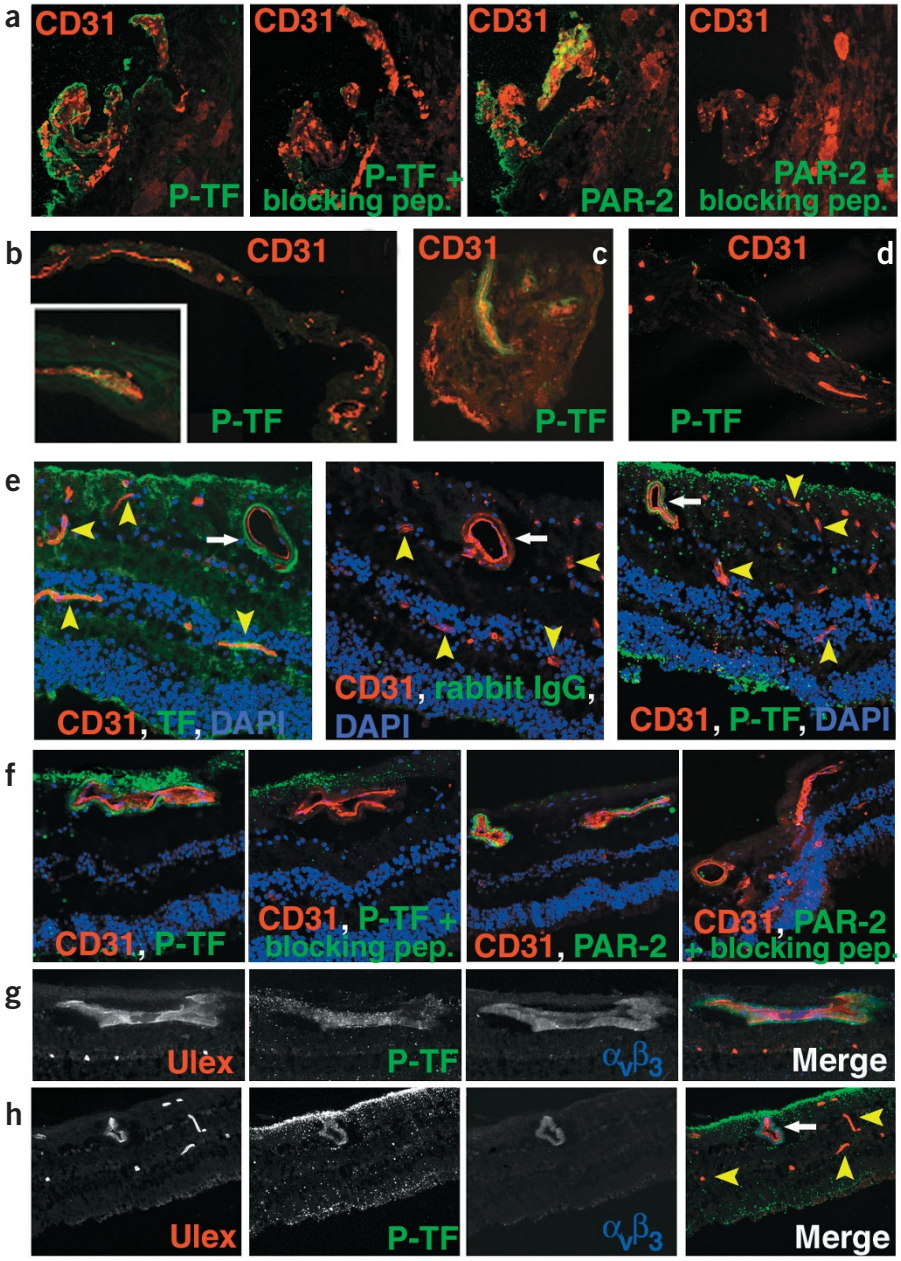

Figure 6 TF phosphorylation and PAR-2 expression in ocular neovascularization. (**a**) Iris specimen from a diabetic patient stained with antibody to Ser258-phosphorylated TF cytoplasmic domain (P-TF) or polyclonal antibody to PAR-2 (confirmed to block PAR-2 cleavage[6]). Peptide immunogen (blocking pep.) was added to confirm specificity. Original magnification, ×20. (**b**,**c**) Additional independent iris specimens from diabetic patients show TF phosphorylation in pathological vessels. **b**, montage of images with ×10 magnification; inset, ×40 magnification. **c**, ×20 magnification. (**d**) Iris specimen from nondiabetic glaucoma patient shows absence of phosphorylated TF. Magnification, ×20. (**e**–**h**) Specimen from patient with clinically diagnosed proliferative diabetic retinopathy. **e**, Staining with polyclonal antibody to TF extracellular domain antibody (TF) shows widespread expression of TF in retina. Pathological (white arrow), but not normal (yellow arrowheads), vessels show staining for phosphorylated TF (×40 magnification). **f**, PAR-2 staining is observed within and adjacent to abnormal retinal neovessels (×40 magnification). **g**,**h**, Phosphorylated TF is localized in abnormal retinal neovessels, confirmed by costaining with LM609 antibody specific for $\alpha_v\beta_3$-integrin[44]. *Ulex europaeus* staining was used as a marker for human endothelial cells. Individual stains are shown without pseudocoloring of fluorescence (white). Pseudocoloring in Merge is indicated by colors of labels in each panel. Magnification, ×40 (**g**) or ×20 (**h**).

marker of vascular proliferation (**Fig. 6g**,**h**). Phosphorylated TF consistently colocalized with $\alpha_v\beta_3$-positive neovessels, whereas normal retinal microvasculature, visualized by *Ulex europaeus* staining, was negative for both (**Fig. 6g**,**h**).

DISCUSSION

Angiogenesis is an important component of the pathology observed in cancer, neovascular eye diseases and arthritis, where activation of coagulation is prevalent[1,2]. In fact, coagulation may indirectly support angiogenesis in several ways, including generation of a transitional fibrin-rich extracellular matrix, release of pro- and antiangiogenic factors from activated platelets, and thrombin signaling through endothelial cell PAR-1 (ref. 17). The results from this study provide new and unexpected insight into how coagulation signaling regulates angiogenesis, by demonstrating that PAR-2 signaling is tightly controlled by the TF cytoplasmic domain. Genetic deletion of the TF cytoplasmic domain results in accelerated physiological and pathological angiogenesis. Thus, loss of negative regulatory control by the TF cytoplasmic domain is a new pathway by which proangiogenic signaling of PAR-2 can be turned on.

Whereas PAR-1 is constitutively expressed in endothelial cells, PAR-2 is specifically upregulated upon inflammatory cytokine stimulation, which also induces TF[32,33]. In addition, TF expression is synergistically enhanced by concomitant VEGF signaling in endothelial cells[33]. Expression of TF and PAR-2, and the functionality of the TF–PAR-2 signaling pathway, thus critically depend on the availability of both angiogenic growth factors and inflammatory cytokines. Inflammatory cytokine production by recruited monocytes and macrophages is recognized as being important for angiogenesis and collateral growth of vessels[34]. These adaptive processes share similarities with wound repair, which is typically associated with efforts by the innate immune system to clear pathogens from injured tissues. Accelerated angiogenesis during wound repair, when there is concomitant inflammation, may be the physiological function of the TF–PAR-2 signaling pathway and, thus, may explain the evolutionary conservation of the TF cytoplasmic domain structure and sites of post-translational modification in vertebrates.

Physiological response pathways frequently cause pathology when negative regulatory control mechanisms are lost. The TF cytoplasmic domain is targeted for post-translational Ser phosphorylation[31,35,36] through PKC-α-dependent pathways in endothelial cells[31]. TF is primarily unphosphorylated, and palmitoylation suppresses agonist-induced TF phosphorylation[31]. We have recently established that

activation of PAR-2, but not PAR-1, leads to phosphorylation of the TF cytoplasmic domain in endothelial cells[37]. Thus, loss of palmitoylation[38] in conjunction with upregulation of PAR-2 determines the degree of phosphorylation of the TF cytoplasmic domain. This concept is supported by *in vivo* data from diabetic eye tissue; we observed a notable colocalization of upregulated PAR-2 with phosphorylated TF only in neovessels. Thus, phosphorylation of TF is the probable mechanism that switches off negative regulatory control to promote pathological PAR-2-dependent angiogenesis.

TF–PAR-2 signaling selectively synergized with PDGF-BB, but not VEGF, basic FGF or PDGF-AA, in TFΔCT aortas. PDGF-BB is readily available, either by release from activated platelets in the context of local coagulation, or by synthesis from sprouting endothelial cells. Although VEGF-targeted antiangiogenic therapy seems efficacious in certain diseases, additional benefit may be obtained from combination therapy with molecules that target alternative and cooperative pathways. Inhibition of PDGF receptors, for example, has synergistic benefit in combination with VEGF-directed approaches[39]. Because PDGF-BB signaling is crucial in stabilizing pericyte recruitment and mature vessel architecture[26,27], generalized PDGF receptor blockade has obvious limitations. For example, reduced vascular pericyte density as a result of endothelium-specific PDGF-BB ablation causes microvascular angiopathy in mice[40]. It may be possible to target deregulated TF cytoplasmic domain signaling to suppress pathological PAR-2- and PDGF-dependent angiogenesis without interfering with the physiological vascular functions of PDGF.

METHODS

Mouse strains and reagents. TFΔCT mice, which lack the 18 C-terminal residues of the TF cytoplasmic domain[41], and PAR-2-deficient mice[42] (provided by P. Andrade-Gordon, Johnson & Johnson Pharmaceutical Research & Development) were backcrossed to yield >90% homogeneity with the C57BL/6 genetic background. TFΔCT PAR-2-deficient double mutants were generated by interbreeding after five generations of backcrossing. Reagents were obtained from the following sources: Matrigel, Becton & Dickinson; endothelial cell growth medium, Clonetics; DMEM, GIBCO; growth factors, R&D Systems; TOPRO and isolectin *Griffonia simplicifolia*, Molecular Probes; antibody to CD31, Santa Cruz; antibodies to SMA and GFAP, Sigma; and antibody to Ki-67, NOVO Laboratories. Goat antibody and monoclonal antibodies to TF, VIIai, hirudin and VIIa were previously described[10]. NAP-c2 and NAP-5 were provided by G. Vlasuk (Corvas International). Adenoviral constructs of human TF(1–263) and human TF(1–243) were previously described[31], and Ad5 serotype vectors coexpressing GFP were similarly generated.

Tumor growth. All animal experiments were approved by the Institutional Animal Care and Use Committee of The Scripps Research Institute. T241 fibrosarcoma cells (4×10^5) were injected subcutaneously into wild-type and TFΔCT mice aged 7–9 weeks and having >97% C57BL/6 genetic background. Tumor volumes and final weights were determined on day 14, and tumors were embedded in OCT. Ten-micron cryosections were fixed with acetone and stained for CD31, and vessel density per microscopic field was determined by fluorescence microscopy from six to eight sections of two tumors each from wild-type and TFΔCT mice.

Angiogenesis assays. The *ex vivo* angiogenesis assay was adopted from the rat aortic sprouting model[18,43]. Thoracic aortas from 8- to 11-week-old wild-type, TFΔCT, PAR-2-deficient and TFΔCT PAR-2-deficient mice of either sex were embedded in Matrigel. Embedded aortas were overlaid with endothelial cell growth medium supplemented with 5% serum and containing growth factors or inhibitors at the following concentrations: VEGF, basic FGF and PDGF, 20 ng/ml; hirudin, 500 nM; VIIai, 100 nM; NAP-c2, 200 nM; NAP-5, 1 μM; and VIIa, 50 nM. In most cases, the number of aortic sprouts was determined on days 3 and 4, without knowledge of the genotype. Aortic ring RNA was isolated by TRIzol (Invitrogen) extraction using standard procedures, digested with DNase I and subjected to RT-PCR for β-actin and TF. Aortic pieces were transduced with adenoviral constructs expressing full-length human TF(1–263) or truncated human TF(1–243) in serum-free DMEM for 20–24 h, before embedding into the sprouting assay. Experiments used two different viral doses, referred to as high (1.1×10^{10} virus particles/ml) and low (5×10^9 particles/ml). For confocal fluorescence microscopy, aortic pieces with a minimum of surrounding Matrigel were fixed with 4% paraformaldehyde and methanol, incubated with primary and secondary antibodies (24 h each) and mounted in anti-fade medium (Vector Laboratories). Alternatively, cryosections of OCT-embedded aortas were fixed with acetone and stained as above.

To evaluate neonatal angiogenesis, retina whole mounts were prepared and angiogenesis was quantified as described[20]. The numbers of retinas and litters used for each genotype were as follows: wild type, 20 retinas from six litters; TFΔCT, 24 retinas from five litters; PAR-2-deficient, 10 retinas from three litters; and TFΔCT PAR-2 deficient, 16 retinas from four litters. Dissected retinas were fixed in 4% paraformaldehyde and methanol, incubated in primary antibody or fluorescence-conjugated isolectin *Griffonia simplicifolia* overnight, incubated with secondary antibody and mounted. All retinas were imaged using the same magnification, resolution and intensity parameters. Images were assembled as single-retina montages, and the diameter of vascularization was quantified using LaserPix software (BioRad; eight diameter measurements taken at one, two, three, four, five and six o'clock, and two random intermediate positions). Total numbers of vascular-related Ki-67$^+$ nuclei were determined by focusing within the vascular plane, which eliminates proliferating neuronal cells from the count.

Analysis of ocular specimens. All experiments using human tissues were performed according to protocols approved by the Human Subjects Committee of the Scripps Office for the Protection of Human Subjects and with permission from informed patients. Specimens of iris, already scheduled to be removed for clinical reasons, were immediately immersed in 20% sucrose at 4 °C before preparation of frozen sections. The specimen of neovascular retina was obtained from the San Diego Eye Bank. This eye was obtained from a patient clinically diagnosed with diabetic retinopathy for over 25 years. After dissection, the retina was fixed with 4% PFA overnight at 4 °C, followed by cryoprotection in 20% sucrose and cryosectioning. Frozen sections were processed for primary antibodies and detected with secondary antibodies conjugated either to Alexa 488, Alexa 568 or Alexa 633 (Molecular Probes) for confocal microscopy. We used mouse antibodies to CD31 (Biocare Medical; 1:50) and $\alpha_v\beta_3$-integrin (LM609; 1:500); rhodamine-conjugated *Ulex europaeus* agglutinin-1 (Vector Laboratories, 1:1,000); and rabbit antibodies to the TF extracellular domain (R4563; 25 μg/ml), Ser258-phosphorylated TF cytoplasmic domain (R6936; 25 μg/ml)[31] and PAR-2 (R6797; 25 μg/ml)[6]. The peptides used as immunogens for R6936 and R6797 were added at 50 μg/ml to confirm specificity.

ACKNOWLEDGMENTS

We thank P. Tejada, A. Donner, and J. Royce for technical assistance; P. Andrade-Gordon for providing PAR-2-deficient mice; and G. Vlasuk for NAP-c2 and NAP-5. M.B. is a fellow of the Medical Faculty, Lund University, Sweden. M.I.D. was supported by Achievement Rewards for Collegiate Scientists. This work was funded by the National Heart Lung Blood Institute (HL-16411 and HL-60742 to W.R.), the National Cancer Institute (CA-85405 to B.M.M.), the National Eye Institute (EY-11254 to M.F.) and the Robert Mealey Program for the Study of Macular Degenerations (to M.F.).

COMPETING INTERESTS STATEMENT

The authors declare that they have no competing financial interests.

Received 14 February; accepted 30 March 2004
Published online at http://www.nature.com/naturemedicine/

1. Folkman, J. Angiogenesis in cancer, vascular, rheumatoid and other disease. *Nat. Med.* **1**, 27–31 (1995).
2. Carmeliet, P. Angiogenesis in health and disease. *Nat. Med.* **9**, 653–660 (2003).
3. Bergers, G., Javaherian, K., Lo, K.M., Folkman, J. & Hanahan, D. Effects of angiogenesis inhibitors on multistage carcinogenesis in mice. *Science* **284**, 808–812 (1999).
4. Kerbel, R. & Folkman, J. Clinical translation of angiogenesis inhibitors. *Nat. Rev. Cancer* **2**, 727–739 (2002).

5. Browder, T., Folkman, J. & Pirie-Shepherd, S. The hemostatic system as a regulator of angiogenesis. *J. Biol. Chem.* **275**, 1521–1524 (2000).
6. Ruf, W., Dorfleutner, A. & Riewald, M. Specificity of coagulation factor signaling. *J. Thromb. Haemost.* **1**, 1495–1503 (2003).
7. O'Brien, P.J., Molino, M., Kahn, M. & Brass, L.F. Protease activated receptors: theme and variations. *Oncogene* **20**, 1570–1581 (2001).
8. Coughlin, S. Thrombin signaling and protease-activated receptors. *Nature* **407**, 258–264 (2000).
9. Camerer, E., Huang, W. & Coughlin, S. R. Tissue factor- and factor X-dependent activation of protease-activated receptor 2 by factor VIIa. *Proc. Natl. Acad. Sci. USA* **97**, 5255–5260 (2000).
10. Riewald, M. & Ruf, W. Mechanistic coupling of protease signaling and initiation of coagulation by tissue factor *Proc. Natl. Acad. Sci. USA* **98**, 7742–7747 (2001).
11. Abe, K. *et al.* Regulation of vascular endothelial growth factor production and angiogenesis by the cytoplasmic tail of tissue factor. *Proc. Natl. Acad. Sci. USA* **96**, 8663–8668 (1999).
12. Bromberg, M.E., Sundaram, R., Homer, R.J., Garen, A., Konigsberg, W.H. Role of tissue factor in metastasis: functions of the cytoplasmic and extracellular domains of the molecule. *Thromb. Haemost.* **82**, 88–92 (1999).
13. Contrino, J., Hair, G., Kreutzer, D.L. & Rickles, F.R. *In situ* detection of tissue factor in vascular endothelial cells: correlation with the malignant phenotype of human breast disease. *Nat. Med.* **2**, 209–215 (1996).
14. Hembrough, T.A. *et al.* Tissue factor/factor VIIa inhibitors block angiogenesis and tumor growth through a nonhemostatic mechanism. *Cancer Res.* **63**, 2997–3000 (2003).
15. Richard, D.E., Vouret-Craviari, V. & Pouysségur, J. Angiogenesis and G-protein-coupled receptors: signals that bridge the gap. *Oncogene* **20**, 1556–1562 (2001).
16. Milia, A.F. *et al.* Protease-activated receptor-2 stimulates angiogenesis and accelerates hemodynamic recovery in a mouse model of hindlimb ischemia. *Circ. Res.* **91**, 346–352 (2002).
17. Griffin, C.T., Srinavasan, Y., Zheng, Y.-W., Huang, W. & Coughlin, S.R. A role for thrombin receptor signaling in endothelial cells during embryonic development. *Science* **293**, 1666–1670 (2001).
18. Masson, V. *et al.* Mouse aortic ring assay: A new approach of the molecular genetics of angiogenesis. *Biol. Proced.* **4**, 24–31 (2002).
19. Siegbahn, A. *et al.* Binding of factor VIIa to tissue factor on human fibroblasts leads to activation of phospholipase C and enhanced PDGF-BB-stimulated chemotaxis. *Blood* **96**, 3452–3458 (2000).
20. Dorrell, M.I., Aguilar, E. & Friedlander, M. Retinal vascular development is mediated by endothelial filopodia, a preexisting astrocytic template and specific R-cadherin adhesion. *Invest. Ophthalmol. Vis. Sci.* **43**, 3500–3510 (2002).
21. Eddleston, M. *et al.* Astrocytes are the primary source of tissue factor in the murine central nervous system: a role for astrocytes in cerebral hemostasis. *J. Clin. Invest.* **92**, 349–358 (1993).
22. Ishida, S. *et al.* Leukocytes mediate retinal vascular remodeling during development and vaso-obliteration in disease. *Nat. Med.* **9**, 781–788 (2003).
23. Ge, L., Ly, Y., Hollenberg, M.D. & DeFea, K. A β-arrestin-dependent scaffold is associated with prolonged MAPK activation in pseudopodia during protease-activated receptor-2 induced chemotaxis. *J. Biol. Chem.* **278**, 34418–34426 (2003).
24. Battegay, E., Rupp, J., Iruela-Arispe, L., Sage, H. & Pech, M. PDGF-BB modulates endothelial proliferation and angiogenesis *in vitro* via PDGF-β receptors. *J. Cell Biol.* **125**, 917–928 (1994).
25. Heldin, C.H. & Westermark, B. Mechanism of action and *in vivo* role of platelet-derived growth factor. *Physiol. Rev.* **79**, 1283–1316 (1999).
26. Uemura, A. *et al.* Recombinant angiopoietin-1 restores higher-order architecture of growing blood vessels in mice in the absence of mural cells. *J. Clin. Invest.* **110**, 1619–1628 (2002).
27. Lindblom, P. *et al.* Endothelial PDGF-B retention is required for proper investment of pericytes in the microvessel wall. *Genes Dev.* **17**, 1835–1840 (2003).
28. Soriano, P. & Hoch, R. Roles of PDGF in animal development. *Development* **130**, 4769–4784 (2003).
29. Jain, R.K. Molecular regulation of vessel maturation. *Nat. Med.* **9**, 685–693 (2003).
30. Carmeliet, P. *et al.* Role of tissue factor in embryonic blood vessel development. *Nature* **383**, 73–75 (1996).
31. Dorfleutner, A. & Ruf, W. Regulation of tissue factor cytoplasmic domain phosphorylation by palmitoylation. *Blood* **102**, 3998–4005 (2003).
32. Nystedt, S., Ramakrishnan, V. & Sundelin, J. The proteinase-activated receptor 2 is induced by inflammatory mediators in human endothelial cells—comparison with the thrombin receptor. *J. Biol. Chem.* **271**, 14910–14915 (1996).
33. Mechtcheriakova, D. *et al.* Specificity, diversity, and convergence in VEGF and TNF-α signaling events leading to tissue factor up-regulation via EGR-1 in endothelial cells. *FASEB J.* **15**, 230–242 (2001).
34. Buschmann, I., Heil, M., Jost, M. & Schaper, W. Influence of inflammatory cytokines on arteriogenesis. *Microcirculation* **10**, 371–339 (2003)
35. Zioncheck, T.F., Roy, S. & Vehar, G.A. The cytoplasmic domain of tissue factor is phosphorylated by a protein kinase C-dependent mechanism. *J. Biol. Chem.* **267**, 3561–3564 (1992).
36. Mody, R.S. & Carson, S.D. Tissue factor cytoplasmic domain peptide is multiply phosphorylated *in vitro*. *Biochemistry* **36**, 7869–7875 (1997).
37. Ahamed, J. & Ruf, W. Protease activated receptor 2 dependent phosphorylation of the tissue factor cytoplasmic domain. *J. Biol. Chem.* published online March 2004 (doi:10.1074/jbc.M401376200).
38. Parat, M.O., Stachowicz, R.Z. & Fox, P.L. Oxidative stress inhibits caveolin-1 palmitoylation and trafficking in endothelial cells. *Biochem J.* **361**, 681–688 (2002).
39. Bergers, G., Song, S., Meyer-Morse, N., Bergsland, E. & Hanahan. D. Benefits of targeting both pericytes and endothelial cells in the tumor vasculature with kinase inhibitors. *J. Clin. Invest.* **111**, 1287–1295 (2003).
40. Enge, M. *et al.* Endothelium-specific platelet-derived growth factor-B ablation mimics diabetic retinopathy. *EMBO J.* **21**, 4307–4316 (2002).
41. Melis, E. *et al.* Targeted deletion of the cytosolic domain of tissue factor in mice does not affect development. *Biochem. Biophys. Res. Comm.* **286**, 580–586 (2001).
42. Damiano, B.P. *et al.* Cardiovascular responses mediated by protease-activated receptor-2 (PAR-2) and thrombin receptor (PAR-1) are distinguished in mice deficient in PAR-2 or PAR-1. *J. Pharmacol. Exp. Ther.* **288**, 671–678 (1999).
43. Nicosia, R.F. & Ottinetti, A. Growth of microvessels in serum-free matrix culture of rat aorta. A quantitative assay of angiogenesis *in vitro*. *Lab Invest.* **63**, 115–122 (1990).
44. Friedlander, M. *et al.* Involvement of integrins $\alpha_v\beta_3$ and $\alpha_v\beta_5$ in ocular neovascular diseases. *Proc. Natl. Acad. Sci. USA* **93**, 9764–9769 (1996).